UTILIZATION OF SENTINEL SATELLITE FOR VERTICAL DEFORMATION MONITORING IN SEMANGKO FAULT-INDONESIA

Atriyon Julzarika [(1); (2)], Harintaka [(1)]

[1] Geodesy Geomatics Engineering, Universitas Gadjah Mada, Jl. Grafika No. 2 Yogyakarta, 55281, Indonesia

[2] Remote Sensing Applications Center, Indonesian National Institute of Aeronautics and Space (LAPAN), Jakarta, 13710, Indonesia

Email: ;verbhakov@yahoo.com; atriyon.julzarika@lapan.go.id; harintaka@ugm.ac.id

KEY WORDS: Sentinel, vertical deformation, DinSAR, Semangko fault, Indonesia

ABSTRACT: Vertical deformation is a change in the surface of the ground that occurs vertically in a certain time. Vertical deformation often occurs in areas with active fault conditions that move vertically or in a mixture. Deformation can be measured by terrestrial or non-terrestrial measurements. One method of non-terrestrial measurement is to use satellite imagery. In this study using Sentinel satellite images. This study aims to utilize Sentinel images in monitoring deformation in the Semangko fault. The Semangko fault is located along the Sumatera island, Indonesia. This fault is one of the most active faults in the world. This fault center is located in the northern part of Lake Singkarak, Tanah Datar Regency. In this region large-scale earthquakes often occur and trigger the movement of faults on other islands and also trigger volcanic activity along the "Barisan Hill" area which is the ring of fire in Sumatera island. Sentinel images can be obtained data every 6-12 days. This facilitates deformation with the differential interferometry SAR (DinSAR) method. Sentinel images used is a minimum of two time periods. Sentinel imagery is suitable for deformation monitoring because the baseline length is >400. Vertical deformation is obtained after the DinSAR process which includes initial correction of image data, interferogram, fringe, phase conversion to height value, and measuring deformation. The results of this vertical deformation can be used for various survey mapping applications such as dynamic DEM, fault mapping, spatial plan, etc.

1. INTRODUCTION

Disasters are events or series of events that threaten and disrupt people's lives and livelihoods caused, both by natural and / or non-natural factors as well as human factors, resulting in human casualties, environmental damage, property losses, and psychological impacts (Martha, Kerle, Jetten, van Westen, & Kumar, 2010). Disaster mitigation according to the disaster law in Indonesia is a series of efforts to reduce disaster risks, both through physical development and awareness raising and capacity to face the threat of disaster (Article 1 paragraph 6 of PP No. 21/2008 concerning the Implementation of Disaster Management).

One of the natural disasters that often occurs in Indonesia is an earthquake. The area that often occurs this disaster is located along the plates, faults, and areas along the ring of fire. Earthquakes occur on the surface of the earth due to the sudden release of energy from the inside which creates seismic waves (Dai et al., 2016). Earthquakes are usually caused by movements of the Earth's crust (Earth's plates) (Hooper, Bekaert, Spaans, & Arikan, 2012). The frequency of an area, refers to the type and size of earthquakes experienced over a period of time (Zuo, Qu, Shan, Zhang, & Song, 2016).

One of the areas that frequently occurs in earthquakes is Sumatera Island, precisely along Bukit Barisan (Barisan Hill). This region is located near the Eurasian plate meeting with IndoAustralia. In addition, Sumatera Island is also passed by one of the most active faults in Indonesia, namely the Semangko fault. In the Semangko fault area there are many volcanoes that form a line. This is the reason why this area is called Bukit Barisan. This fault has caused the formation of large lakes on Sumatra island, including a combination of tectonic and volcanic activity. The lakes are Lake Singkarak, Lake Maninjau, Lake Toba, Lake Kerinci, Lake Air Tawar, Lake Diatas, Lake Dibawah, and Lake Ranau(Julzarika et al., 2018). Even though this area is very tectonically active, there are still very few tools for monitoring. Deformation measuring devices are only installed at several points. Monitoring of tectonic deformation and volcanic deformation in the Semangko fault is still rare. Monitoring deformation at the Semangko fault is one aspect of utilizing survey mapping survey in the field of disaster.

Deformation can be measured by terrestrial or non-terrestrial measurements (Amighpey & Arabi, 2016). One method of non-terrestrial measurement is to use satellite imagery. Nowadays the use of satellite imagery in Indonesia has been used for variety of mapping applications, such as disasters, environmental natural resources, and defense and security (Zhang et al., 2019). In this study using X SAR and Sentinel satellite images. Synthetic Aperture Radar (SAR) images will be useful in predicting deformation in an area. The advantages obtained in the form of deformation with high degree of precision (Rucci, Ferretti, Monti Guarnieri, & Rocca, 2012). The results of measurements with this SAR image can be obtained high accuracy when compared with terrestrial deformation measurements. This study aims to utilize Sentinel images in monitoring deformation in the Semangko fault.

2. METHOD

This section discusses the area of study and the methods used and the data used. The study area is located in the Semangko Fault. The chosen method is interferometry.

2.1 Semangko faults

The Semangko fault is a geological formation along the Sumatera island (Geological, 2017). This fault stretches from Aceh in the north to south in Semangka Bay, Lampung (Mukti, 2018). This fault forms the Bukit Barisan. Semangko fault is relatively young. This fault can be seen directly in the Sianok canyon and Anai Valley, West Sumatera. This fault is a sliding fault, like the San Andreas fault in California. The Semangko Fault is located between the Semangko Fault Zone of Lampung. The southern part of the Semangko block is divided into landscapes such as the Semangko mountains, the Ulehbeluh and Walima Depression, the Horst Ratai and the Belitung Bay Depression. While the northern part of the Semangko block is shaped like a Dome (diameter +40 Km). The Semangko Fault is thought to have formed millions of years ago when the Indian-Australian Plate (Ocean) crashed across the western part of Sumatera which was part of the Eurasian Plate (Continent) (Hurukawa, Wulandari, & Kasahara, 2014).

Geologist Katili in The Great Sumatran Fault (1967) said, these cracks formed in the Middle Miocene period or about 13 million years ago (Katili & A., 1967). The western plate of the Semangko Fault moves northwest at a speed of 10 mm / year to 30 mm / year relative to the eastern part. The Semangko Fault Field is a subduction zone to a depth of 10-20 km tightly locked so that pressure accumulation occurs (Geological, 2017; Mukti, 2018).

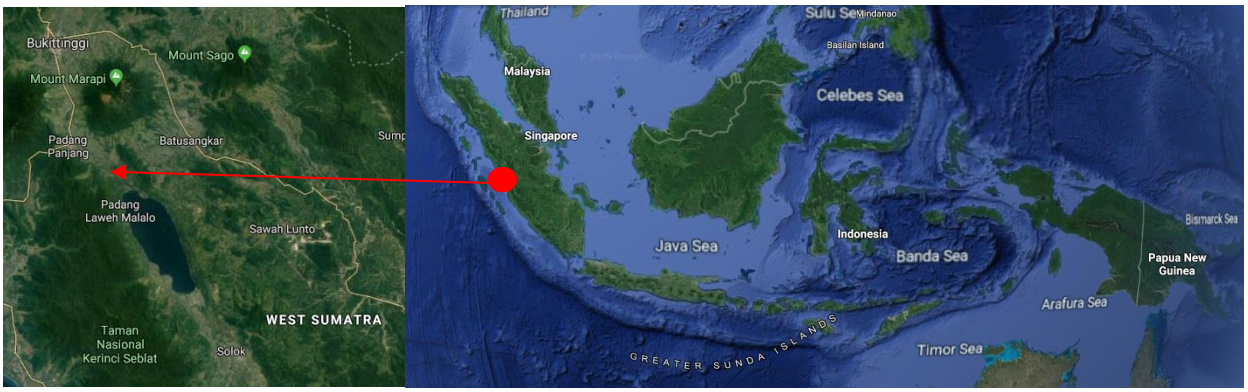

Figure 1. Study area in Semangko Fault, northern of Lake Singkarak, West Sumatera

In this study, the Semangko fault area studied was in the northern part of Lake Singkarak, Tanah Datar Regency, West Sumatra Province, see Figure 1. This area is the main center of the Semangko fault where this region often experiences earthquakes and affects other areas on Sumatera island and its surroundings. The earthquake in this tectonic region that caused the formation of Lake Singkarak. This lake has endemic flora and fauna and is a world tourist location of diverse and interesting topography.

2.2 Interferometry, DInSAR, and Deformation

INSAR is a remote sensing technology that uses radar image sensors from aircraft or satellites (Julzarika & Susanto, 2009; Nico, Leva, Fortuny-Guasch, Tarchi, & Antonello, 2005) or techniques used to extract three-dimensional (3D) information from the Earth's surface by observing the phase of radar waves (Pieraccini & Miccinesi, 2019). IFSAR uses differences in phase measurements to obtain distance differences and distance changes from two or more SAR images that have complex values from the same surface(Monserrat, Crosetto, & Luzi, 2014). The resulting difference from this phase results in a new image type (Leberl, 1984). The difference is called an interferogram(Ruiz-Armenteros et al., 2018); (Caro Cuenca, Hooper, & Hanssen, 2013). This interferogram has a pattern of color circles (edges) in the form of surface topography (Crosetto, Monserrat, Cuevas-González, Devanthéry, & Crippa, 2016).

DInSAR is a SAR interferometry method used to monitor deformation from a minimum of two INSAR data and in a certain time. DINSAR can be obtained from the difference of two DTMs from INSAR or it can also be done by interferometry processing of 4 time-difference SAR data. DSM is an elevation model that includes the roof of buildings, trees and other objects, usually as a canopy model (Li, Zhu, & Gold, 2004). DEM is a model of bare earth elevation or surface autocorrelation without vegetation, buildings, and other objects [103]. DTM is a DEM that has been equipped with rivers, contours, and features that exist in nature (Li et al., 2004).

Deformation is a change in the shape, position, and dimensions of an object (Kuang, 1996). Deformation can be interpreted as a change in the position or movement of a point in an object in absolute or relative terms. Deformation is a part of geodynamics. Deformation can be known from the deformation survey and geodetic survey. Vertical deformation is a change in the surface of the ground that occurs vertically in a certain time. Vertical deformation often occurs in areas with active fault conditions that move vertically or in a mixture.

2.3 X SAR dan Sentinel

X SAR is a satellite image of *Deutches fur Luft und Raumfarht* (DLR). This image has a resolution of 1 arc second (Hoja & D'Angelo, 2010)(DLR, 2010). X SAR has an X band so that it will produce a more optimal DSM. One product of X SAR is SRTM X. In this study, X SAR data is used as a starting point for deformation of the Sentinel deformation. Sentinel is a European Space Agency (ESA) natural resource satellite. This satellite consists of several types, namely Sentinel 1 (SAR), Sentinel 2 (optical), and Sentinel 3 (microwave) (ESA, 2019). Sentinel 1 Satellite can be used for monitoring vertical deformation with INSAR. The Sentinel 2 satellite can be used for horizontal deformation monitoring.

3. RESULT AND DISCUSSION

Monitoring of deformation on the Semangko fault was carried out in three steps, namely the extraction of DSM and DTM in 2000, the extraction of DSM and DTM with Sentinel in 2018, and calculating the vertical deformation from 2000 to 2018.

3.1 The extraction of DSM2000 and DTM2000

The X SAR data used is in the form of an interferogram obtained from the DLR. This interferogram data is carried out by various interferometry processing processes until it is converted to height points. This height points are interpolated between points until the DSM is obtained by using an ellipsoid reference. After that the geoid undulation correction is done with Earth Gravitational Model (EGM) 2008. This global geoid model is used in Indonesian regions due to the availability of rare and not free local geoid data in Indonesia. DSM with the EGM2008 geoid field is then called the DSM2000, see Figure 2.

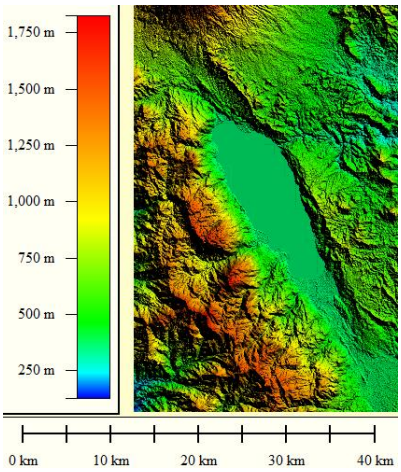

Figure 2. DSM2000

This DSM2000 is done height error correction so that DSM2000 is free from pits and spires. Then DSM2000 was corrected by DSM2DTM method with the aim of getting DTM2000. This method is an converting DSM to be DTM using least square adjustment (Julzarika & Sudarsono, 2009). The parameters considered in the conversion of DSM to DTM are the viewpoint of the top of the vegetation and the radius of 11 pixels from the pixel's central point on DSM2000. The DTM2000 also needs height error correction. Figure 3 is DTM2000. The DTM2000 still uses the EGM2008 reference field.

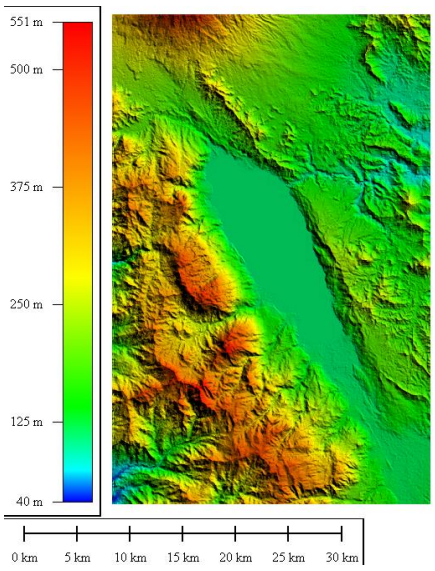

Figure 3. DTM2000

The DTM2008 is used as a reference basis for calculating deformation of the deformation data from Sentinel. The deformation is compared with DTM2018. DSM2000 can be used as a basis for calculating changes in vegetation height for DSM2018.

3.2 DSM2018 and DTM2018

DSM2018 was made using the interferometry method. Sentinel data are used in two time periods in 2018 with a difference of 3 months. This interferometry method includes importing additional data and information, coregistration of Sentinel images, preprocessing, interferogram and calculating coherence, interferogram filtration, phase unwrapping, absolute to high phase, high matrix geocoding. The unwrapping phase is an absolute phase matrix. In the absolute high matrix phase on the ground coordinate system. In geocoding, the absolute high relative matrix in the high projection system. The high reference field used in this interferometry is EGM2008. This geoid model was chosen so that it has the same height reference field as DSM2000. This interferometry will produce DSM which still have high errors. The DSM needs to be done with pits and spires removal with height error correction. The result obtained is DSM2018, see Figure 4. Figure 4 is DSM 2018 obtained from the results of interferometry.

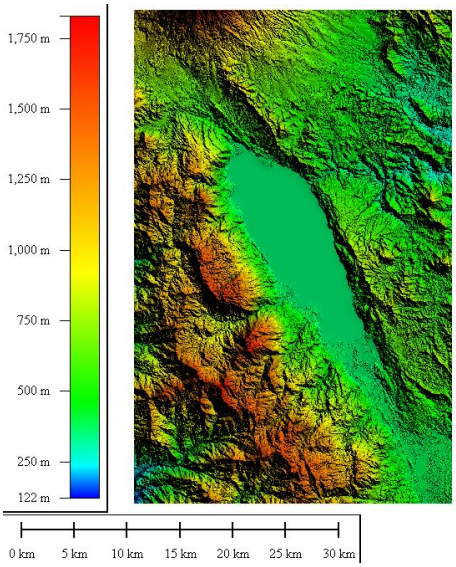

Figure 4. DSM2018, extracted from Sentinel interferometry

The next step is making DTM2018 by filtering DSM2018. The parameters used are the viewpoint of the top of the vegetation and the radius of 11 pixels from the pixel's central point on DSM2018. This parameter selection is the same as DTM2000 in order to get the same treatment. The DTM obtained also needs height error correction. The tolerance used for height errors in this study was 1.96σ with a confidence level of 95%. This tolerance is also treated equally on DSM2000, DTM2000, and DSM2018. Figure 5 is DTM2018.

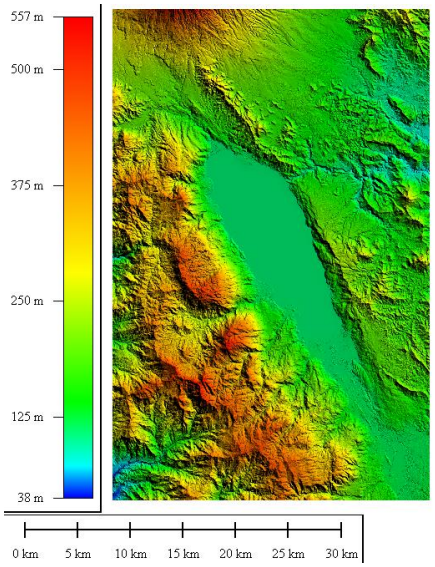

Figure 5. DTM2018

3.3 Vertical deformation in 2000=20018

DSM2000, DTM2000, DSM2018, and DTM2018 have been successfully obtained with height error free conditions. Next is the detection of vertical deformation that occurs in the Semangko Fault region. Vertical deformation can be detected by subtracting DTM2000 from DTM2018. This method is one of the quick ways to minimize processing time and mapping costs in Indonesia. This method is an alternative other than Differential

Interferometry SAR (DInSAR), Persistant Scatter (PS)-INSAR, or other methods that are still not optimal for rapid mapping on Sumatera island. Figure 6 is the result of a vertical deformation in 2000-2018 in Semangko fault.

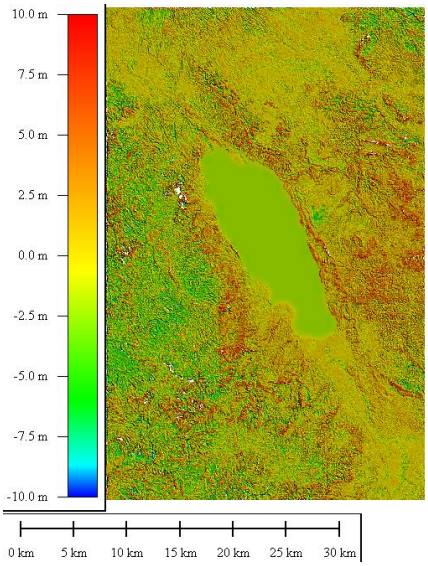

Figure 6. vertical deformation from 2000 to 2018

In that region the deformation that occurs is equal to + 10 m. Generally areas with 5-10 m vertical deformation are caused by landslides during earthquakes or rain with high intensity. Overall vertical deformation that occurred from 2000 to 2018 is + 3 m. If the average is done then the deformation around the center of the Semangko fault is 15.79 cm / year. This value is an approximate value from satellite mapping and this value is relative. The quality of the results of this mapping can be done in 2 ways namely height difference test and Root Means Square (RMSE) on field measurements. Height difference test was carried out on DTM2000 and DTM2018. The smaller or close to 0 the number of differences in height the higher the accuracy and the value of the vertical deformation bias will be smaller.

DSM2000 and DSM2018 can be used for calculating changes in vegetation height. The way to do this is to subtract DSM2018 with DSM2000. The result of this difference is the difference in surface height difference. The surface can be natural objects and artificial objects. Natural objects such as vegetation, rivers while artificial objects such as settlements, roads, and other human-made objects. Figure 7 is a surface height change from 2000 to 2018.

Field measurements include height and deformation measurements with Geodetic GNSS -leveling. There are 5 five points around the Semangko Fault north of Lake Singkarak that have been measured. The measured point can be seen in the following Table 1. The measured points are compared with the height points on DTM2018. The results obtained are the five points have height difference of.ground measurement.

Table 1. height points and ground measurement

No	Latitude	Longitude	H (ground) (m)	H(2000) (m)	H(2018) (m)	dh1 (m)	dh2 (m)	information
1.	0° 32' 44.79" S	100° 31' 37.62" E	111,6	112,66	111,03	-1,059	0,569	Down movement
2.	0° 31' 39.49" S	100° 29' 16.25" E	114.2	118,12	113,93	-3,922	0,274	Down movement
3.	0° 30' 20.70" S	100° 27' 22.88" E	160.3	161,76	159,09	-1,465	1,21	Down movement
4.	0° 33' 20.66" S	100° 28' 48.03" E	134.8	134,6	134.90	0,2	-0,103	Up movement
5.	0° 28' 27.99" S	100° 28' 22.83" E	223.4	224.26	223.09	-0,857	0,313	Down movement

dh1 is H(ground)-H(2000) , dh2 is H(ground)-H(2018)

Based on the results of the ground measurements, the results show that the height points value with GNSS-leveling The difference between the height of the field point and the height in 2000 and height in 2018 is not too significant. In general, the difference in field measurement points with DTM2018 is 0.2 - 0.5 m. The difference in field measurement points with DTM2000 is 0.2-3.5. This study area generally experiences in down movement. This comparison and its measurement using 1,96σ (95 %) (ASPRS, 2014).

DSM2000 and DSM2018 can be used for calculating changes in vegetation height. The way to do this is to subtract DSM2018 with DSM2000. The result of this difference is the difference in surface height difference. The surface can be natural objects and artificial objects. Natural objects such as vegetation, rivers while artificial objects such as settlements, roads, and other human-made objects. Figure 7 is a picture of the surface height change from 2000 to 2018.

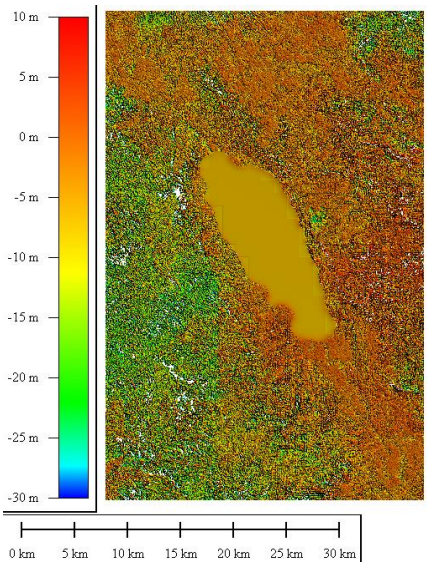

Figure 7. DTM2008

Changes in vegetation and non-vegetation height from 2000 to 2018. Changes detected were around 10 meters of deformation. If the change is increase (+), an increase in vegetation height occurs. If the change is valuable decrease (-) a reduction in vegetation height occurs.

4. CONCLUSION

This study has the conclusion that vertical deformation monitoring in the Semangko Fault can use X SAR and Sentinel satellite images. Vertical deformations monitored were from 2000 to 2016. Image X SAR of 2000 was used for the extraction of DSM2000 and DTM2000. Sentinel imagery is used for DSM2018 and DTM2018 extraction. Vertical deformation obtained at 15.79 cm/year. The vertical deformation was obtained from the reduction of DTM2018 with DTM2000. In addition to vertical deformation, surface height changes (vegetation and non-vegetation) can also be obtained from the result of reducing DSM2018 with DSM2000. Surface changes are detected by an average of ~ + 10 m.

5. ACKNOWLEDGEMENT

Thank to Gadjah Mada University (UGM), LAPAN, Tanah Datar Regency Regency, DLR, and ESA for the support of research and data used.

6. REFERENCES

Amighpey, M., & Arabi, S. (2016). Studying land subsidence in Yazd province, Iran, by integration of InSAR and levelling measurements. *Remote Sensing Applications: Society and Environment*, *4*. https://doi.org/10.1016/j.rsase.2016.04.001

ASPRS. ASPRS Accuracy Standards for Digital Geospatial Data, The American Society for Photogrammetry and Remote Sensing § (2014). https://doi.org/10.1016/S0033-3506(98)80082-6

Caro Cuenca, M., Hooper, A. J., & Hanssen, R. F. (2013). Surface deformation induced by water influx in the abandoned coal mines in Limburg, The Netherlands observed by satellite radar interferometry. *Journal of Applied Geophysics*, *88*, 1–11. https://doi.org/10.1016/j.jappgeo.2012.10.003

Crosetto, M., Monserrat, O., Cuevas-González, M., Devanthéry, N., & Crippa, B. (2016). Persistent Scatterer Interferometry: A review. *ISPRS Journal of Photogrammetry and Remote Sensing*, *115*, 78–89. https://doi.org/10.1016/j.isprsjprs.2015.10.011

Dai, K., Li, Z., Tomás, R., Liu, G., Yu, B., Wang, X., … Stockamp, J. (2016). Monitoring activity at the Daguangbao mega-landslide (China) using Sentinel-1 TOPS time series interferometry. *Remote Sensing of Environment*, *186*, 501–513. https://doi.org/10.1016/j.rse.2016.09.009

DLR. (2010). DLR SRTM Digital Elevation Models, 10–11.

ESA. (2019). Sentinel Satellites. Retrieved from https://www.esa.int/Our_Activities/Observing_the_Earth/Copernicus/Overview4

Geological. (2017). Sesar Semangko. Retrieved from http://geologicalmelankolia.blogspot.com/2017/03/sesar-semangko-sumatera.html

Hoja, D., & D'Angelo, P. (2010). Analysis of DEM combination methods using high resolution optical stereo imagery and interferometric SAR data. *International Archives of the Photogrammetry, Remote Sensing and Spatial Information Science,Volume XXXVIII,Part 1*, 02–05. https://doi.org/10.1007/978-3-319-59489-7

Hooper, A., Bekaert, D., Spaans, K., & Arikan, M. (2012). Recent advances in SAR interferometry time series analysis for measuring crustal deformation. *Tectonophysics*, *514–517*, 1–13. https://doi.org/10.1016/j.tecto.2011.10.013

Hurukawa, N., Wulandari, B. R., & Kasahara, M. (2014). Earthquake history of the Sumatran fault, Indonesia, since

1892, derived from relocation of large earthquakes. *Bulletin of the Seismological Society of America*, *104*(4), 1750–1762. https://doi.org/10.1785/0120130201

Julzarika, A., Laksono, D. P., Subehi, L., Dewi, E. K., Kayat, K., Sofiyuddin, H. A., & Nugraha, M. F. I. (2018). Comprehensive integration system of saltwater environment on Rote Island using a multidisciplinary approach. *J. Degrade. Min. Land Manage*, *5*(53), 2502–2458. https://doi.org/10.15243/jdmlm

Julzarika, A., & Sudarsono, B. (2009). PENURUNAN MODEL PERMUKAAN DIJITAL (DSM) MENJADI MODEL ELEVASI DIJITAL (DEM) DARI CITRA SATELIT ALOS PALSAR (Studi kasus: NAD Bagian Tenggara, Indonesia) Atriyon Julzarika *), Bambang Sudarsono **). *Jurnal Teknik*, *30* no *1*, 57–63. https://doi.org/https://doi.org/10.14710/teknik.v30i1.1814

Julzarika, A., & Susanto, S. (2009). PEMANFAATAN INTERFEROMETRIC SYNTHETIC APERTURE RADAR (InSAR) UNTUK PEMODELAN 3D (DSM, DEM, DAN DTM). *Majalah Sains Dan Teknologi Dirgantara Desember*, *4*(4), 154–159.

Katili, & A., J. (1967). On the occurrence of Large Transcurrent Faults in Sumatra, Indonesia. *J. Geosciences Osaka City Univ.*, *10*, 5–17. Retrieved from http://ci.nii.ac.jp/naid/10012396688/en/

Kuang, S. (1996). *Geodetic network analysis and optimal design : concepts and applications*. Chelsea, Mich.: Ann Arbor Press.

Leberl, F. W. (1984). A review of: " Microwave Remote Sensing—Active and Passive ". By F. T. Ulaby. R. K. Moore and A. K. Fung. (Reading, Massachusetts: Addison-Wesley, 1981 and 1982.) Volume I: Microwave Remote Sensing Fundamentals and Radiometry. [Pp. 473.] Price U.S. $46.5. *International Journal of Remote Sensing*, *5*(2), 463–463. https://doi.org/10.1080/01431168408948820

Li, Z., Zhu, Q., & Gold, C. (2004). *Digital terrain modeling: Principles and methodology*. *Digital Terrain Modeling: Principles and Methodology*. https://doi.org/10.1201/9780203357132

Martha, T. R., Kerle, N., Jetten, V., van Westen, C. J., & Kumar, K. V. (2010). Characterising spectral, spatial and morphometric properties of landslides for semi-automatic detection using object-oriented methods. *Geomorphology*, *116*(1–2), 24–36. https://doi.org/10.1016/j.geomorph.2009.10.004

Monserrat, O., Crosetto, M., & Luzi, G. (2014). ISPRS Journal of Photogrammetry and Remote Sensing A review of ground-based SAR interferometry for deformation measurement. *ISPRS Journal of Photogrammetry and Remote Sensing*, *93*, 40–48. https://doi.org/10.1016/j.isprsjprs.2014.04.001

Mukti, M. M. (2018). STRUCTURAL CONFIGURATION AND DEPOSITIONAL HISTORY OF THE SEMANGKO PULL-APART BASIN IN THE SOUTHEASTERN SEGMENT OF SUMATRA FAULT ZONE. *RISET*, *28*(1), 115–128. https://doi.org/10.14203/risetgeotam2018.v28.954

Nico, G., Leva, D., Fortuny-Guasch, J., Tarchi, D., & Antonello, G. (2005). Generation of digital terrain models with a ground-based SAR system. *IEEE Transactions on Geoscience and Remote Sensing*, *43*(1), 45–49. https://doi.org/10.1109/TGRS.2004.838354

Pieraccini, M., & Miccinesi, L. (2019). Ground-based radar interferometry: A bibliographic review. *Remote Sensing*, *11*(9). https://doi.org/10.3390/rs11091029

Rucci, A., Ferretti, A., Monti Guarnieri, A., & Rocca, F. (2012). Sentinel 1 SAR interferometry applications: The outlook for sub millimeter measurements. *Remote Sensing of Environment*. https://doi.org/10.1016/j.rse.2011.09.030

Ruiz-Armenteros, A. M., Lazecky, M., Ruiz-Constán, A., Bakoň, M., Delgado, J. M., Sousa, J. J., … Perissin, D. (2018). Monitoring continuous subsidence in the Costa del Sol (Málaga province, southern Spanish coast) using ERS-1/2, Envisat, and Sentinel-1A/B SAR interferometry. *Procedia Computer Science*, *138*, 354–361. https://doi.org/10.1016/j.procs.2018.10.050

Zhang, B., Wang, R., Deng, Y., Ma, P., Lin, H., & Wang, J. (2019). Mapping the Yellow River Delta land subsidence with multitemporal SAR interferometry by exploiting both persistent and distributed scatterers. *ISPRS Journal of Photogrammetry and Remote Sensing*, *148*(October 2018), 157–173. https://doi.org/10.1016/j.isprsjprs.2018.12.008

Zuo, R., Qu, C., Shan, X. J., Zhang, G., & Song, X. (2016). Coseismic deformation fields and a fault slip model for the Mw7.8 mainshock and Mw7.3 aftershock of the Gorkha-Nepal 2015 earthquake derived from Sentinel-1A SAR interferometry. *Tectonophysics*, *686*, 158–169. https://doi.org/10.1016/j.tecto.2016.07.032